

Structural anomalies at the magnetic and ferroelectric transitions in RMn_2O_5 ($R=Tb, Dy, Ho$)C. R. dela Cruz,¹ F. Yen,¹ B. Lorenz,¹ M. M. Gospodinov,² C. W. Chu,^{1,3,4} W. Ratcliff,⁵ J. W. Lynn,⁵ S. Park,⁶ and S.-W. Cheong⁶¹*Department of Physics and TCSUH, University of Houston, Houston, Texas 77204-5002, USA*²*Institute of Solid State Physics, Bulgarian Academy of Sciences, 1784 Sofia, Bulgaria*³*Lawrence Berkeley National Laboratory, 1 Cyclotron Road, Berkeley, California 94720, USA*⁴*Hong Kong University of Science and Technology, Hong Kong, China*⁵*NIST Center for Neutron Research, NIST, Gaithersburg, Maryland 20899, USA*⁶*Department of Physics & Astronomy and Rutgers Center for Emergent Materials, Rutgers University, Piscataway, New Jersey 08854, USA*

(Received 11 January 2006; revised manuscript received 1 March 2006; published 20 March 2006)

Strong anomalies of the thermal expansion coefficients at the magnetic and ferroelectric transitions have been detected in multiferroic RMn_2O_5 . Their correlation with anomalies of the specific heat and the dielectric constant is discussed. The results provide evidence for the magnetic origin of the ferroelectricity mediated by strong spin-lattice coupling in the compounds. Neutron scattering data for $HoMn_2O_5$ indicate a spin reorientation at the two low-temperature phase transitions.

DOI: [10.1103/PhysRevB.73.100406](https://doi.org/10.1103/PhysRevB.73.100406)

PACS number(s): 75.25.+z, 75.80.+q, 77.80.-e, 65.40.De

Frustrated magnetic systems have recently attracted the attention of solid state physicists with regard to the observed magnetoelectric couplings and the induced ferroelectricity in some orthorhombic rare earth manganites^{1–5} and other frustrated compounds.⁶ These materials are of fundamental interest since it has been demonstrated that an external magnetic field can rotate the ferroelectric (FE) polarization.^{3,6,7} Despite intense experimental investigations, the physical origin of the large magnetoelectric coupling and the ferroelectricity arising at the magnetic lock-in transitions is not yet understood. The giant magneto-dielectric effects and the ferroelectricity in these compounds require the existence of sizable atomic displacements and structural distortions, the magnetic origin of which is believed to lie in extraordinarily strong spin-lattice interactions. The experimental verification of these structural anomalies is essential to prove the suggested intimate correlation between the magnetic and FE orders.

The search for structural distortions by neutron scattering experiments have indicated some anomalies in the temperature dependence of the lattice parameters of $TbMn_2O_5$ (Ref. 8) and $DyMn_2O_5$,⁹ however, due to the limited resolution of such scattering experiments a unique assignment to the various phase transitions in these compounds appears extremely difficult. Other investigations of $HoMn_2O_5$ (Ref. 9) and YMn_2O_5 (Refs. 4 and 10) have failed completely to resolve structural anomalies. It is, therefore, one of the key issues to detect and to characterize the structural distortions in RMn_2O_5 manganites giving rise to ferroelectricity and to investigate the coupling between magnetic, dielectric, and lattice degrees of freedom.

In this Rapid Communication we present our results of high-resolution thermal expansion measurements along the three crystallographic orientations in RMn_2O_5 ($R=Ho, Dy, Tb$). Sharp structural anomalies are detected at all magnetic and FE phase transitions, the strongest anomalies appearing at the transitions into the FE phases associated with a significant change of the electric polarization. Single

crystals of RMn_2O_5 have been prepared by the high-temperature solution growth method as described elsewhere.^{2,11} Thermal expansion measurements were conducted employing a high-resolution capacitance dilatometer. The experimental techniques have been described earlier.¹² With our current device we achieved a resolution (above the noise level) of 4 Å. The expansion data were correlated to anomalies of the b -axis dielectric constant and the heat capacity measured for the same crystals.

In orthorhombic RMn_2O_5 the spins of the Mn^{4+} and Mn^{3+} ions and the R^{3+} moments are coupled via the predominantly antiferromagnetic (AFM) superexchange interactions giving rise to a complex magnetic phase diagram.⁹ The common features for all RMn_2O_5 are a transition into a high-temperature Néel phase (HTIC) with a two-component incommensurate (IC) magnetic modulation characterized by a wave vector $\vec{q}=(q_x, 0, q_z)$ at $T_{N1} \approx 43$ K followed by a lock-in transition into a commensurate (CM) phase with $\vec{q}=(0.5, 0, 0.25)$ at T_{C1} only a few degrees lower where the ferroelectricity arises. With further decreasing temperature, at T_{C2} , the CM phase becomes unstable towards a low-temperature IC phase (LTIC) with a magnetic modulation $\vec{q} \approx (0.48, 0, 0.3)$.^{5,8–10,13,14} The transition at T_{C2} is accompanied by a significant decrease of the FE polarization and is often referred to as a second FE phase transition. In some rare earth compounds (e.g., $HoMn_2O_5$, $DyMn_2O_5$) additional anomalies have been observed indicating an even more complex magnetic structure that has yet to be explored.^{11,15}

It is characteristic for all RMn_2O_5 compounds that the various magnetic phase changes are reflected in sharp and distinct anomalies of the dielectric constant, as shown in Figs. 1(a), 2(a), and 3(a) for $R=Ho, Dy$, and Tb . This is a clear indication of strong magnetoelectric coupling due to large spin-lattice interactions. The thermodynamic signature of the various transitions is obvious from the peaks of the specific heat C_p , Figs. 1(a), 2(a), and 3(a). Several transitions show pronounced hysteresis effects, not shown in the figures

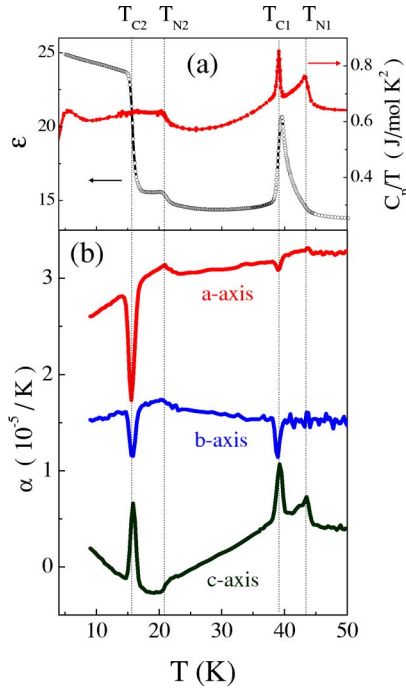


FIG. 1. (Color online) Anomalies at the magnetic phase transitions in HoMn₂O₅. The transition temperatures are marked by vertical dotted lines. Only warming data are shown in all figures. (a) Dielectric constant along b (open circles, left scale) and specific heat (closed circles, right scale). (b) Thermal expansivities along a , b , and c axes. For better clarity the data along a and b axes are offset by 2.6 and 1.4 units, respectively.

(for enhanced clarity only warming data are included in Figs. 1–4). The thermal expansivities, displayed in Figs. 1(b), 2(b), and 3(b), exhibit distinct anomalies at all magnetic transitions. Our data provide striking evidence for the existence of extraordinarily large spin-lattice interactions in RMn₂O₅ resulting in macroscopic displacements along all three crystallographic axes. They further prove that the magnetic and lattice degrees of freedom are strongly coupled and the simultaneous magnetic and FE transitions at T_{C1} and T_{C2} have to be considered as the phase change of one highly correlated system.

The thermal expansion data for the three manganites ($R = \text{Ho, Dy, Tb}$) exhibit similarities but also distinct differences depending on the rare earth ion. The changes of the lattice parameters have to be discussed with respect to the magnetic orders derived from neutron scattering experiments.^{8,9,13–15} The first transition from the paramagnetic (PM) and paraelectric (PE) phase into the HTIC phase at $T_{N1} \approx 43$ K is characterized by a peak of C_p , an increase of ϵ , and a sudden increase of the expansivities along a and c axes. Considering the spiral IC magnetic order below T_{N1} with the wave vector $\vec{q} = (0.5 + \beta, 0, 0.25 + \delta)$, the increase of α_a and α_c with the onset of AFM order can be explained by the magnetoelastic effect. There is no anomaly of α_b which is consistent with the lack of the magnetic modulation along b .

The FE transition at T_{C1} coincides with the lock-in of the magnetic wave vector into commensurate values. It is well

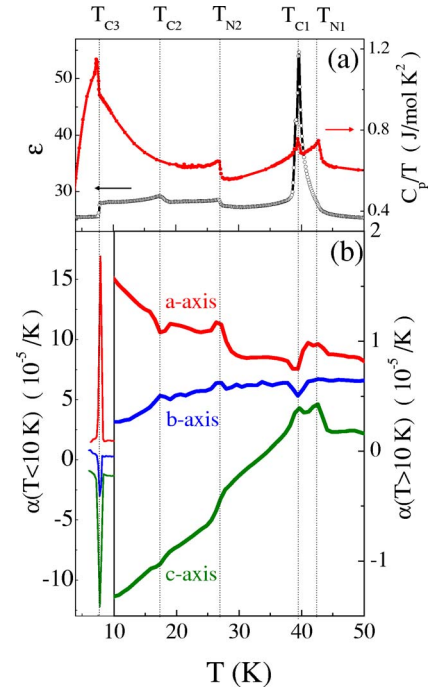


FIG. 2. (Color online) Same as Fig. 1 for DyMn₂O₅. The b -axis expansivity is offset by 0.6 units. Note the different scales (left and right) chosen for the expansivities below and above 10 K, respectively.

marked by sharp peaks of C_p and ϵ as well as strong peaks of the expansivities along all three axes (Figs. 1–3). We define the abrupt length change ΔL at the transition as the difference of the lengths in the low- and high-temperature phases extrapolated to $T \geq T_C$ and $T \leq T_C$, respectively. The mea-

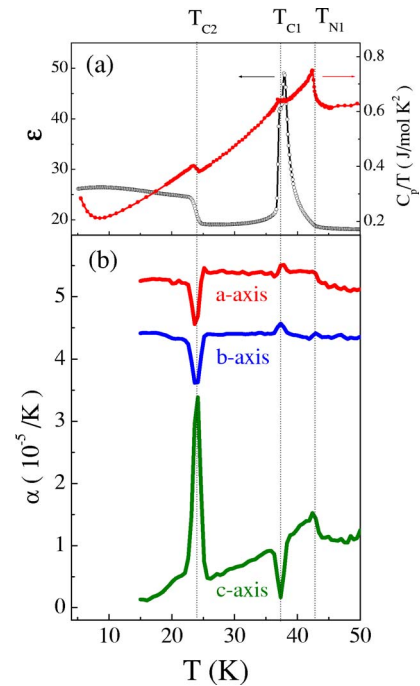


FIG. 3. (Color online) Same as Fig. 1 for TbMn₂O₅. The a - and b -axis expansivities are offset by 5 and 4.2 units, respectively.

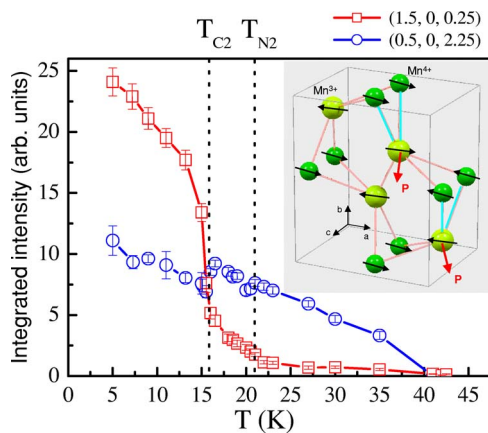


FIG. 4. (Color online) Integrated intensities of two neutron scattering peaks of HoMn_2O_5 along different directions in reciprocal space. Inset: Mn-spin configuration in the CM phase below T_{C1} .

sured values for ΔL along a , b , and c are listed in Table I. For $R=\text{Ho}$ and Dy the c axis contracts while a and b expand at T_{C1} [Figs. 1(b) and 2(b)]. However, the opposite is observed for $R=\text{Tb}$ [Fig. 3(b)]. This behavior has its origin in the different spin modulations along c , given by $q_z=0.25+\delta$. For Ho and Dy δ is negative^{9,15} but for Tb δ is positive.^{8,14} The length change of the c axis is directly correlated with the deviation of the magnetic wavelength λ_m along c from its commensurate value of $4c$. The spin-lattice coupling leads to an attraction between the IC spin wave and the underlying lattice period along c between T_{N1} and T_{C1} resulting in a stress on the lattice. This stress is tensile for $R=\text{Ho}, \text{Dy}$ ($\lambda_m > 4c$) but compressive for $R=\text{Tb}$ ($\lambda_m < 4c$). At the lock-in transition the stress is suddenly released ($\lambda_m = 4c$) resulting in an abrupt decrease (increase) of c for $R=\text{Ho}, \text{Dy}$ (Tb). This transition at T_{C1} is of first order as indicated by the volume change derived from the expansion data, the jump of q_x and q_z ,¹⁴ and the thermal hysteresis observed in $\varepsilon(T)$. Mediated by the elastic forces of the lattice, a and b contract (Tb) or expand (Ho, Dy) opposite to c . In Ho and TbMn_2O_5 the length change along c dominates whereas in DyMn_2O_5 it is rather minor (Table I). This qualitative difference has its origin in the Mn^{4+} spin alignment along c that polarizes the rare earth moments. For $R=\text{Ho}, \text{Tb}$ there are alternating FM and AFM links along c that may cause a positional modulation of R and the connecting oxygen, $\text{O}(2)$, which is seen in α_c at T_{C1} whereas in DyMn_2O_5 the Mn^{4+} spins are only FM along c and the expansion anomaly is accordingly small.⁹ Strong lattice anomalies have also been observed in GdMnO_3 at the transition into the FE phase that

happens in this multiferroic compound at higher magnetic fields.¹⁶

The superexchange interactions between neighboring Mn^{3+} and Mn^{4+} ions in the a - b plane are all AFM and the smallest closed loop of neighboring Mn spins involves five ions. Therefore, magnetic frustration must exist as, for example, revealed by the spin order in HoMn_2O_5 displayed in the inset of Fig. 4.⁹ The spins of two Mn^{3+} per unit cell are each frustrated with two neighboring Mn^{4+} with the same spin direction. Reducing this frustration by moving the two Mn^{3+} away from the Mn^{4+} (along the arrows labeled \mathbf{P} in Fig. 4) generates a dipolar moment \mathbf{P} between the Mn^{3+} and the surrounding oxygen ions. The a components of \mathbf{P} cancel out while the b components add up to the macroscopic polarization along b and ferroelectricity. The proposed displacement lowers the symmetry to $\text{Pb}2_1m$. This empirical picture is supported by recent Mössbauer experiments on YMn_2O_5 showing that neighboring Mn^{3+} ions are magnetically inequivalent.¹⁷ The corresponding displacement vector of only two of the four Mn^{3+} is a superposition of the basis vectors of the Γ_{1g} and Γ_{3u} irreducible representations of the space group $Pbam$ in contrast to the model proposed for YMn_2O_5 where the displacement of all four Mn^{3+} ions was assumed (Γ_{3u} representation).⁴ We would like to emphasize that the AFM modulation along a with $q_x=0.5$ is crucial for the above discussion, as it leads to the frustration and displacement of both Mn^{3+} and the net polarization along b . Considering the role of magnetic frustration to stabilize ferroelectricity in RMn_2O_5 there are interesting similarities to multiferroic $\text{Ni}_3\text{V}_2\text{O}_8$ and TbMnO_3 . For the latter compounds it was shown that the transition from sinusoidal to helical magnetic modulation can introduce a third order coupling giving rise to FE order.^{6,18} By symmetry the same argument holds also for two noncollinear spin density waves with the same propagation vector but different phases.¹⁹ In fact, neutron scattering experiments have revealed the existence of a noncollinear spin structure in RMn_2O_5 ($R=\text{Ho}, \text{Dy}, \text{Tb}$) (Ref. 9) with \vec{q} along the a axis which shows that the ferroelectricity below T_{C1} is not forbidden by symmetry. However, it is not clear yet if the magnetic structure between T_{C1} and T_{N1} is sinusoidal and the transition into the FE phase follows the same mechanisms as in $\text{Ni}_3\text{V}_2\text{O}_8$ or TbMnO_3 . Furthermore, the magnetic modulation in the FE phase of RMn_2O_5 is commensurate whereas it is incommensurate in $\text{Ni}_3\text{V}_2\text{O}_8$ or TbMnO_3 .

The FE transition at T_{C1} is followed by additional phase changes at lower T as indicated by characteristic changes of ε and C_p and distinct anomalies of the expansion coefficients (Figs. 1–3). For $R=\text{Ho}$ and Dy a steplike increase of both ε

TABLE I. Relative change of lattice parameters at the FE transitions in RMn_2O_5 . $\Delta L=L(T < T_C) - L(T > T_C)$.

$\Delta L/L$ ($\times 10^{-6}$)	HoMn_2O_5		DyMn_2O_5		TbMn_2O_5	
	T_{C1}	T_{C2}	T_{C1}	T_{C3}	T_{C1}	T_{C2}
$\Delta a/a$	2.1	13.4	3.8	-67.1	-1.1	11.3
$\Delta b/b$	2.5	5.7	2.0	16.3	-2.0	11.5
$\Delta c/c$	-6.6	-8.3	-2.0	63.0	10.2	-41.5

and C_p at $T_{N2}=22$ and 27 K, respectively, is followed by another increase of ε at $T_{C2}=16$ K (Ho) and 17 K (Dy) with a significant change of the FE polarization.² The ε anomaly at T_{C2} is largest in HoMn_2O_5 but there is no equivalent signature in C_p of $\text{Ho(Dy)Mn}_2\text{O}_5$. Recent neutron scattering experiments on DyMn_2O_5 indicate that a spin reorientation takes place at T_{N2} and also at T_{C2} .¹⁵ Our neutron scattering results shown in Fig. 4 provide clear evidence for spin reorientations in HoMn_2O_5 at T_{N2} and T_{C2} . The integrated intensity of the (1.5,0,0.25) peak suddenly increases at both transitions whereas that of the (0.5,0,2.25) peak shows a sharp drop. The details of the magnetic orders in the various phases have yet to be determined. In TbMn_2O_5 the spin reorientation transition at T_{N2} appears to be missing, however, from the distinct step of C_p at 24 K (similar to the C_p anomalies in Ho and DyMn_2O_5 at T_{N2}) we conclude that this transition coincides with the FE transition at T_{C2} (determined by the sharp increase of ε).

The FE transition at T_{C2} is accompanied by another change of the magnetic modulation that becomes incommensurate again, $\vec{q} \approx (0.48, 0, 0.3)$ (LTIC phase). The strongest anomalies of the expansion coefficients appear at T_{C2} for $R = \text{Ho}$ and Tb (Figs. 1 and 3, Table I) indicating a sizable distortion of the lattice due to the $\text{CM} \rightarrow \text{LTIC}$ phase change. The corresponding anomalies are less pronounced in DyMn_2O_5 (Fig. 2). Instead, another low- T transition at $T_{C3} = 7.5$ K is associated with giant changes of the lattice constants, a large contraction of the a axis, and an expansion of b and c (Table I). This phase transition is the onset of strong AFM order of the Dy moments along a [$\vec{q}_{(\text{Dy})} = (0.5, 0, 0)$] (Ref. 15), and the a contraction is explained by large mag-

netostrictive effects. C_p exhibits a sharp peak at T_{C3} and ε drops to its high-temperature value ($T > T_{N1}$). It was suggested that the low- T state in DyMn_2O_5 is paraelectric²⁰ and it appears conceivable that the lattice strain below T_{C3} is dominated by the Dy order, as evidenced by the huge expansion anomalies at T_{C3} . The AFM order of the Dy moments with $q_x=0.5$ appears to dominate the low-temperature magnetic structure and the associated lattice distortions, which could explain the PE low- T phase in DyMn_2O_5 . However, neutron scattering experiments have found that the Dy magnetic order coexists with the CM and IC orders of the Mn spins¹⁵ and further investigations are needed for a final conclusion.

The strongest lattice anomalies observed in our thermal expansion measurements occur at the FE transitions involving a significant change of the polarization. They are highly anisotropic and prove the existence of an extraordinarily strong spin-lattice coupling. The magnetic and FE orders have to be considered as one highly correlated system that is coupled by magnetoelastic interactions.

ACKNOWLEDGMENTS

This work was supported in part by NSF Grant No. DMR-9804325, the T.L.L. Temple Foundation, the J. J. and R. Moores Endowment, and the State of Texas through the TCSUH and at LBNL by the DOE. The work of M. M. G. was supported by the Bulgarian Science Foundation, Grant No. F 1207. The work at Rutgers was supported by NSF, Grant No. DMR-0080008.

¹T. Kimura, G. Lawes, T. Goto, Y. Tokura, and A. P. Ramirez, Phys. Rev. B **71**, 224425 (2005).

²N. Hur, S. Park, P. A. Sharma, S. Guha, and S.-W. Cheong, Phys. Rev. Lett. **93**, 107207 (2004).

³N. Hur, S. Park, P. A. Sharma, J. S. Ahn, S. Guha, and S.-W. Cheong, Nature (London) **429**, 392 (2004).

⁴I. Kagomiya, S. Matsumoto, K. Kohn, Y. Fukuda, T. Shoubu, H. Kimura, Y. Noda, and N. Ikeda, Ferroelectrics **286**, 167 (2003).

⁵S. Kobayashi, H. Kimura, Y. Noda, and K. Kohn, J. Phys. Soc. Jpn. **74**, 468 (2005).

⁶G. Lawes, A. B. Harris, T. Kimura, N. Rogado, R. J. Cava, A. Aharony, O. Entin-Wohlman, T. Yildirim, M. Kenzelmann, C. Broholm, and A. P. Ramirez, Phys. Rev. Lett. **95**, 087205 (2005).

⁷T. Kimura, T. Goto, H. Shintani, K. Ishizaka, T. Arima, and Y. Tokura, Nature (London) **426**, 55 (2003).

⁸L. C. Chapon, G. R. Blake, M. J. Gutmann, S. Park, N. Hur, P. G. Radaelli, and S.-W. Cheong, Phys. Rev. Lett. **93**, 177402 (2004).

⁹G. R. Blake, L. C. Chapon, P. G. Radaelli, S. Park, N. Hur, S.-W. Cheong, and J. Rodriguez-Carvajal, Phys. Rev. B **71**, 214402 (2005).

¹⁰S. Kobayashi, T. Osawa, H. Kimura, Y. Noda, I. Kagomiya, and

K. Kohn, J. Phys. Soc. Jpn. **73**, 1593 (2004).

¹¹B. Mihailova, M. M. Gospodinov, B. Güttler, F. Yen, A. P. Litvinchuk, and M. N. Iliev, Phys. Rev. B **71**, 172301 (2005).

¹²T. H. Johansen, J. Feder, and T. Jossang, Rev. Sci. Instrum. **57**, 1168 (1986).

¹³C. Wilkinson, F. Sinclair, P. Gardner, J. B. Forsyth, and B. M. R. Wanklyn, J. Phys. C **14**, 1671 (1981).

¹⁴S. Kobayashi, T. Osawa, H. Kimura, Y. Noda, N. Kasahara, S. Mitsuda, and K. Kohn, J. Phys. Soc. Jpn. **73**, 3439 (2004).

¹⁵W. Ratcliff II, V. Kiryukhin, M. Kenzelmann, S.-H. Lee, R. Erwin, J. Schefer, N. Hur, S. Park, and S.-W. Cheong, Phys. Rev. B **72**, 060407(R) (2005).

¹⁶J. Baier, D. Meier, K. Berggold, J. Hemberger, A. Balbashov, J. A. Mydosh, and T. Lorenz, Phys. Rev. B **73**, 100402(R) (2006).

¹⁷I. Kagomiya, S. Nakamura, S. Matsumoto, M. Tanaka, and K. Kohn, J. Phys. Soc. Jpn. **74**, 450 (2005).

¹⁸M. Kenzelmann, A. B. Harris, S. Jonas, C. Broholm, J. Schefer, S. B. Kim, C. L. Zhang, S.-W. Cheong, O. P. Vajk, and J. W. Lynn, Phys. Rev. Lett. **95**, 087206 (2005).

¹⁹M. Mostovoy, Phys. Rev. Lett. **96**, 067601 (2006).

²⁰D. Higashiyama, S. Miyasaka, N. Kida, T. Arima, and Y. Tokura, Phys. Rev. B **70**, 174405 (2004).